Title

Provision of secondary frequency regulation by coordinated dispatch of industrial loads and thermal power plants

Authors

Bao, Yi
Xu, Jian
Feng, Wei
et al.

Publication Date

2019-05-01

DOI

10.1016/j.apenergy.2019.03.025

Peer reviewed

Applied Energy 241 (2019) 302–312

Contents lists available at ScienceDirect

Applied Energy

journal homepage: www.elsevier.com/locate/apenergy

Provision of secondary frequency regulation by coordinated dispatch of industrial loads and thermal power plants☆

Yi Bao[a], Jian Xu[a,*], Wei Feng[b], Yuanzhang Sun[a], Siyang Liao[a], Rongxin Yin[b], Yazhou Jiang[c], Ming Jin[d], Chris Marnay[b]

[a] Wuhan University, Wuhan, Hubei Province 430072, China
[b] Energy Technologies Area, Lawrence Berkeley National Laboratory, 1 Cyclotron Road, Berkeley, CA 94720, USA
[c] GE Global Research Center, Niskayuan, NY 12309, USA
[d] University of California Berkeley, Berkeley, CA 94720, USA

HIGHLIGHTS

- The flexibility of industrial parks is leveraged for frequency regulation.
- The stochastic day-head optimization is transformed into deterministic.
- An economic model predictive control is used to enhance the profit and performance.
- The proposed hierarchical framework is verified based on a real-world power market.

ARTICLE INFO

Keywords:
Demand response
Economic model predictive control
Frequency regulation
Hierarchical control
Industrial parks
Load control

ABSTRACT

Demand responsive industrial loads with high thermal inertia have potential to provide ancillary service for frequency regulation in the power market. To capture the benefit, this study proposes a new hierarchical framework to coordinate the demand responsive industrial loads with thermal power plants in an industrial park for secondary frequency control. In the proposed framework, demand responsive loads and generating resources are coordinated for optimal dispatch in two-time scales: (1) the regulation reserve of the industrial park is optimally scheduled in a day-ahead manner. The stochastic regulation signal is replaced by the specific extremely trajectories. Furthermore, the extremely trajectories are achieved by the day-ahead predicted regulation mileage. The resulting benefit is to transform the stochastic reserve scheduling problem into a deterministic optimization; (2) a model predictive control strategy is proposed to dispatch the industry park in real time with an objective to maximize the revenue. The proposed technology is tested using a real-world industrial electrolysis power system based upon Pennsylvania, Jersey, and Maryland (PJM) power market. Various scenarios are simulated to study the performance of the proposed approach to enable industry parks to provide ancillary service into the power market. The simulation results indicate that an industrial park with a capacity of 500 MW can provide up to 40 MW ancillary service for participation in the secondary frequency regulation. The proposed strategy is demonstrated to be capable of maintaining the economic and secure operation of the industrial park while satisfying performance requirements from the real world regulation market.

1. Introduction

To achieve a sustainable and clean energy system of the future, governments together with the industry are putting efforts to promote the integration of renewable with an emphasis on integration of wind and solar into the power grid. The intermittency and variation of renewable by nature expose power grid to numerous operational challenges. The resulting threat on system reliability and resilience has drawn attention from legislators as well as power industry all over the world and corresponding policies have been put in place to enhance the

☆ This work was supported in part by the Natural Key R&D Program of China (2017YFB0902900), in part by the Natural Science Foundation of Hubei Province, China (No. 2018CFA080) and in part by the National Natural Science Foundation of China (No. 51707136).

* Corresponding author.
E-mail address: xujian@whu.edu.cn (J. Xu).

https://doi.org/10.1016/j.apenergy.2019.03.025
Received 26 October 2018; Received in revised form 27 January 2019; Accepted 5 March 2019
Available online 12 March 2019
0306-2619/

Nomenclature

H	set of hours
T	set of time slots in one hour
I	set of generators
J	set of industrial loads
h	index of an hour in set H
t	index of a time slot in set T
i	index of generators
j	index of ASLs
N1	horizon of reserve scheduling
N2	prediction horizon of MPC
$\text{Income}^{\text{day}}$	daily income of the industrial park
$\text{Income}^{\text{product}}$	daily income of the industrial loads
$\text{Income}^{\text{regualtion}}$	daily income of the frequency regulation
$\text{Cost}^{\text{generation}}$	daily operation cost of thermal power plants industrial loads
$\text{Penalty}^{\text{regulation}}$	daily penalty for frequency regulation
π_h^{perf}	price of regulation performance at hour h
R_h^{reg}	benefits factor of regulation at hour h
K_h^{perf}	performance score of regulation at hour h
$\pi_h^{product}$	price of the aluminum products at hour h ($/Ton)
$\eta_h^{product}$	power consumption rate for aluminum products (ton/MW)
$c_h^{generation}$	fuel cost of the thermal power plant at hour h
$a_1 - a_3$	parameters of the generator fuel cost function
$\eta_h^{regulation}$	penalty coefficient of regulation at hour h
$P_{eco,j}^{load}$	baseline power output of ASL j
$P_{\min,j}^{load}$	minimum power output of ASL j
$P_{\max,j}^{load}$	maximum power output of ASL j
$P_{eco,i}^{generator}$	baseline power of generator i
$P_{\min,i}^{generator}$	minimum power output of generator i
$P_{\max,i}^{generator}$	minimum power output of generator i
$\beta_{up,j}^{load}$	maximum ramping up rate of ASL j
$\beta_{down,j}^{load}$	maximum ramping down rate of ASL j
$\beta_{up,i}^{generator}$	minimum ramping up the rate of generator i
$\beta_{down,i}^{generator}$	minimum ramping down the rate of generator i
$P_{h,j,t}^{load}$	output power of ASL k in time slot t at hour h
$P_{h,i,t}^{generator}$	output power of generator i in time slot t at hour h
$\omega_{h,t}$	regulation signal in time slot t at hour h
Ω	trajectories contain different numbers of deviation
B	different bins of regulation mileage
$T_{t,i}$	time constant of the turbine of generator i
$T_{g,i}$	time constant of the governor of generator i
M	inertia constant of the industrial park
D	load damping constant of the industrial park
$\Delta P_{m,i}$	incremental mechanical power of generator i
$\Delta P_{g,i}$	incremental value gate position of generator i
$\Delta P_{C,i}$	frequency control signal of generator i
Δf_i	incremental frequency of generator i
ΔP_L	incremental load demand
ΔP_{tie}	incremental tie-line power
T_{tie}	interconnection gain between an industrial park and bulk grid
$\Delta P_{ASL,j}$	incremental power of ASL j
ΔP_{CL}	incremental power of conventional loads
x	vector of industrial park states
u	vector of industrial park control input
w	disturbance
A, B, C, E	system matrices of industrial parks state space
A_d, B_d, C_d, E_d	discrete system matrices of industrial parks state space
Q_{reg}	weighting matrices corresponding to the regulation profit
Q_G	weighting matrices corresponding to generators energy losses
Q_{ASL}	weighting matrices corresponding to the ASL products loss
$Q_{vpenalty}$	weighting matrices corresponding to the variation penalty
$Q_{overpenalty}$	weighting matrices corresponding to the regulation penalty
$u_{G\min}, u_{G\max}$	amplitude constrains of control variables of generators
$u_{ASL\min}, u_{ASL\max}$	amplitude constrains of control variables of ASLs
$\Delta x_{G\min}, \Delta x_{G\max}$	ramping constraints of states variables of generators
$u_{ASL\min}, u_{ASL\max}$	ramping constraints of states variables of ASLs

flexibility of power systems for high penetrations of renewable. In the United States, Federal Energy Regulatory Commission (FERC) issued Order 755 to promote demand-side resources to participate in frequency regulation markets [1]. The National Grid in the United Kingdom (UK) has developed a dynamic frequency service named Enhanced Frequency Response (EFR) to improve the management of system frequency [2]. Even though China is still in an early development phase of frequency regulation market, the Chinese government has issued a notice encouraging electric energy storage resources [3] as well as large industrial loads such as steel industry loads [4] to participate in frequency regulation markets. All these orders mandate demand-side resources to be fairly compensated in frequency markets, which makes demand-side resources competitive compared to conventional generation for the provision of secondary frequency control.

Resources for frequency regulation are generally required to follow random regulation signals in a timely manner. State-of-the-art research on demand responsive resources to participate in frequency regulation is mainly focused on residential and commercial loads, i.e., electric vehicles (EVs) [5–8], energy storage system [9], heating ventilation and air-conditioning (HVAC) systems [10,11], and other thermostatically controlled loads (TCLs) [12]. The flexibility of electric vehicles (EVs) is leveraged for primary regulation in [5], secondary frequency regulation in [6] and emergency frequency regulation services in [7] respectively. Furthermore, an on-going EV vehicle-to-grid demonstration project is developed for frequency regulation in [8]. An investigation into how energy storage can fulfill the fast frequency response is considered in [9]. Experimental evaluation of frequency regulation from HVAC is verified in [10]. The potential of TCLs for frequency regulation is calculated in [11] and field experiment with TCLs to study frequency control is presented [12]. However, due to the sparseness and a limited capacity, residential loads or commercial loads have to be aggregated in a large scale for frequency control, and the requirement of an aggregator and the communication delay between the aggregator and the distributed load may affect the effectiveness to meet the regulation performance for frequency control.

Different from residential and commercial loads, energy-intensive industrial loads are advantageous to provide this frequency regulation ancillary service in that: (1) Industrial loads can provide a large amount of ancillary service due to an enormous power capacity (a series of industrial loads' power capacity can be up to 1000 MW); (2) Industrial loads are equipped with advanced infrastructures which enable a central controller to dispatch demand-responsive assets to follow regulation signals; (3) Industrial loads have substantial thermal mass, which allows for instantaneous power change following a regulation signal without significantly impacting the quality of electricity service; (4) Industrial loads are operated continuously with high cyclicality, thereby offering reliable sources for frequency regulation; (5) Industrial loads have self-owned thermal power plants, which can be coordinated with demand responsive loads to further leverage the flexibility from industrial loads for up and down regulation reserve.

Over the last decade, extensive research has been conducted on demand response for frequency regulation in power systems. Ref. [13]

demonstrated that industrial loads with a large storage capacity or fuel-switching capability are able to provide frequency regulation service. These loads include data centers, industrial electrolysis, industrial cement, pulp mills, arc furnaces, steel rolling loads and electric boilers. In [14], data center loads are regarded as a source of dynamic flexibility for primary regulation and a joint power management strategy of a data center and plug-in electric vehicles for frequency regulation is studied in [15]. To avoid the discreteness of crushers in the cement industry and pulp in the paper industry, a coordinated framework with energy storage is proposed in [16] that improves frequency regulation performance. Among the various types of industrial loads, industrial electrolysis is demonstrated to be able to provide more flexibility to support system operation. Minute-to-minute regulation of electrolysis aluminum loads is achieved in [17] by manually controlling the ratio of the voltage-regulating transformer. A frequency feedback control framework is proposed to allow aluminum smelter loads (ASLs) for system frequency control in an isolated power system by controlling the generator's excitation voltage [18,19] or the saturation reactor of the ASL [20]. Based on this architecture, experimental verification of ASLs for frequency regulation is reported in [21,22] based on the real-world isolated power system. The flexibility of industrial loads, especially industrial electrolysis loads is proven for frequency control while the flexibility of up reserves has not been fully investigated.

Apart from flexibility, industrial regulation resources are required to determine their optimal regulation capacity over a multi-hour operation within the constraints of market timelines [23]. The challenge is to determine the optimal regulation reserve considering the uncertainty from market prices and regulation signals in the day-ahead market. To manage this uncertainty, the research explored the stochasticity [24–26] of the resources or managed the risk robustly in a deterministic framework [27–29]. In [24], a stochastic algorithm is developed for frequency control with a consideration of the randomness of prices and the regulation signal. Reference [25] proposed a bidding algorithm for the aggregator to participate in the day-ahead market based on stochastic optimization. Based on stochastic programming with a set of possible price curves, [26] proposes an optimal bidding strategy to maximize regulation revenues. The uncertainty of the regulation signal is verified by the worst-case trajectories in [27]. Based on this robust optimization framework, the regulation resources succeed in following the uncertain signal reliably for most of the time. A robust optimization framework that models the regulation signal as energy constrained is proposed in [28,29]. Furthermore, experimental verification is conducted to verify the effectiveness of the robust framework in [30,31]. However, the aforementioned work is based on the premise that regulation resources respond quickly to follow the regulation signal and the regulation capacity is small. Since industrial loads have an enormous regulation capability, the uncertainty of the regulation signal will have a more significant influence on the performance of the industrial loads for frequency regulation.

In addition to the day-ahead regulation reserve schedule, a real-time regulation strategy to track the regulation signal while maintaining economic and secure operation of the industrial loads is in a critical need. A large number of literature have explored the strategy based on model predictive control (MPC) for real-time regulation control. In [32], an MPC strategy is presented for tracking the frequency signal by groups of EVs, controllable loads, and cogeneration power plants. A framework based on a decentralized MPC is proposed in [33] to coordinate the generator and EVs in a three-area interconnected power system. However, economic factors during the regulation process or the correlation between day-ahead optimal reserve scheduling and real-time regulation have not been considered. The economic MPC (EMPC) with an objective to directly reflect process economics is proposed in [34]. The application of EMPC is utilized in the chemical process [35], and the power management [36], but a few kinds of literature report its application for frequency regulation.

To bridge the gap, this paper proposes a hierarchical control framework built upon the work in [30] to explore industrial parks for participation in frequency regulation. In the proposed framework, it considers the slow dynamic process of industrial loads and thermal power plants together with the fact that the random regulation signal has a more severe impact on the profits of the industrial parks. Different from [30] which assumes HVAC can quickly track the regulation signal, energy and production loss and the regulation penalty are incorporated during the regulation process in this study. The main contributions of this study are as follows:

(1) a coordinated scheme of the self-owned thermal power plant and the industrial loads is proposed to enhance the flexibility of industrial parks for frequency regulation. By complementary the large regulation capability of thermal power plants with the fast regulation ability of industrial loads, the industrial park is able to provide a high-quality regulation service in the power market.

(2) a hierarchical control framework is proposed to enable industrial parks to fully achieve their flexibility to provide ancillary service for frequency regulation. In the day-ahead ancillary market, the stochastic regulation signal is replaced by the specific extremely trajectories. Furthermore, the extremely trajectories are achieved by the day-ahead predicted regulation mileage. The resulting benefit is to transform the stochastic reserve scheduling problem into a deterministic optimization. In the real-time dispatch, the economic model predictive control with a cost function of the regulation process is proposed to maximize the potential revenue during regulation. In addition, the control scheme considers the correlation of the day-ahead regulation reserve schedule and real-time regulation operation.

2. Typical industrial park and provision framework statement

2.1. Power system topology of the industrial park

An industrial park is a zone area composed of energy-intensive industrial consumers, e.g., industrial electrolysis and the steel industry. The annual energy consumption of these industrial loads is up to 14.49MWHr per ton so that industrial parks must utilize self-owned thermal power plants for part of their electricity supply while the bulk grid provides additional electricity through the transmission line. The typical topology of an industrial park is shown in Fig. 1.

The potential flexibility of industrial parks is promising since the power output of industrial loads, especially electrolysis loads, is flat without much fluctuation. Further, each industrial park as shown in Table 1 generally has a large capacity to provide a regulation reserve. This kind of industrial parks is widely distributed in the developing country where the frequency regulation markets considering industrial parks are not available. To study the feasibility of leveraging flexible industrial parks for frequency regulation, regulation requirements of the PJM market is used. In this study, we focus on electrolysis loads, e.g., electrolytic aluminum, electrolytic zinc, and electrolytic copper for secondary frequency control. The flexibility of other loads will be studied in the future.

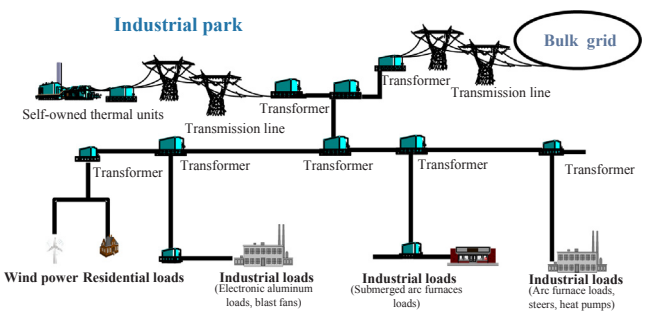

Fig. 1. Diagram of an industrial park network.

Table 1
Capacity of typical industrial parks.

Typical industrial park	Capacity (MW)	Productivity (ton)	Power consumption (kWh/ton)
Electrolytic aluminum	1360	895,000	13,307
Electrolytic copper	100	250,000	97.4
Electrolytic zinc	300	150,000	342.8
Steel plant	1300	13,390,000	667.9

2.2. Problem statement and framework provision

This paper focuses on leveraging the flexibility of industrial parks to provide frequency regulation service. The objective is to maximize the potential profit during the frequency regulation process while providing a high quality of regulation service. However, this is a challenging task due to several factors: (1) the independent system operator (ISO) requires symmetric regulation reserves, i.e., up-regulation reserves and down-regulation reserves. However, the flexibility of industrial loads is limited by the rated capabilities of the electric equipment. Hence, coordination between industrial loads and thermal power plants is vital to ensure the industry parks meet the symmetric regulation requirement; (2) the regulation signal is unpredictable in the day-ahead market, which increases the difficulty in determination of the optimal regulation scheduling; (3) since the provision of frequency regulation often requires industrial loads to deviate from normal operation, the penalty associated with load deviation needs to be considered; (4) the production benefits of loads are satisfied so as to track the regulation signal. As a result, there exists a tradeoff between regulation performance and regulation benefits in real-time regulation. (5) Since the predictive error in the day-ahead market influences the real-time operation, how to consider the day-ahead predictive error in real-time operation remains to be solved.

To solve the aforementioned challenges, this study develops a hierarchical controller as shown in Fig. 2. The controller consists of two-time scales: day-ahead ancillary service market and real-time optimal dispatch of industrial parks. The day-ahead ancillary market determines the optimal regulation reserve offered by the industrial park to ISO/RTO, which is aimed to deal with challenges 1 and 2; The real-time dispatch of industrial parks tracks ISO's frequency regulation signal while maintaining the economic operation of the load during the real-time operation, which addresses challenges 3 and 4; The hierarchical framework solves the challenge 5. The details of each level are presented in Section 3 and Section 4, respectively.

3. Day-ahead level reserve optimization

3.1. Stochastic regulation reserve optimization formulation

3.1.1. Objective function

In this section, the regulation reserve of industrial parks is optimized with an objective to maximize the potential revenue. We denote the operation time horizon, the set of thermal power plants and the set of ASLs by $H = \{1, ...,h\}$, $I = \{1, ...,i\}$, and $J = \{1, ...,j\}$, respectively. Each hour is divided into multiple time slots as $T = \{1, ...,t\}$. Each time slot corresponds to the day-ahead calculate time step. For an industrial park, the total daily income denoted as $\text{Income}^{\text{day}}$, is calculated by:

$$\max\ \text{Income}^{\text{day}} = \sum_{h\in H}(\text{Income}_h^{product} + \text{Income}_h^{regulation} - \text{Cost}_h^{generation} - Penalty_h^{regulation}) \quad (1)$$

where $Income^{product}$ denotes the revenue from the industrial load's daily production, $Income_h^{regulation}$ is the revenue from the regulation ancillary service within hour h, $Cost_h^{generation}$ represents the generators' operation cost within hour h, and $Penalty_h^{regulation}$ denotes the penalty of loads for overloading within hour h.

The product income $Income^{product}$ is determined by:

$$\text{Income}_h^{product} = \sum_{j\in J}\left[\pi_h^{product}\cdot\eta_h^{product}\cdot\sum_{t\in T}P_{h,j,t}^{load}\Delta t\right],\ \forall\ h,\ j,\ t \quad (2)$$

where $\pi_h^{production}$ denotes the unit revenue of the aluminum products, $\eta_h^{production}$ is the constant power consumption rate for aluminum products, and P_h^{load} represents the operational power demand of the ASLs products.

The regulation revenue $Income_h^{regulation}$ consists of two parts, i.e., the capability payment and the performance payment, which is formulated as:

$$\text{Income}_h^{regulation} = (\pi_h^{cap} + \pi_h^{perf}\cdot R)\cdot K^{perf}\cdot r_t^{reg},\ \forall\ h,\ t \quad (3)$$

where π_h^{cap} is the regulation market capability clearing price, π_h^{perf} is the regulation market performance clearing price and r_k^{reg} denotes the regulation capacity. K^{perf} denotes the performance score, which reflects the accuracy of the regulation resource's response to the regulation signal. PJM calculates the performance score as the hourly average of three components, the correlation score, the delayed score, and the precision score [36]. R denotes the mileage factor that converts the dynamic regulation signal (RegD) into the traditional regulation signal (RegA). In PJM, the mileage factor R is approximately 2.92.

A quadratic cost function is typically used to denote the cost of thermal generation in the industrial park [38], which is formulated as:

$$\text{Cost}_h^{generation} = \sum_{i\in I}\sum_{t\in T}[c_h^{genaration}\cdot(\alpha_1 P_{h,i,t}^{g2} + \alpha_2 P_{h,i,t}^{g} + \alpha_3)\Delta t],\ \forall\ h,\ i,\ t \quad (4)$$

where $c_h^{generation}$ denotes the fuel cost of the thermal unit and $[\alpha_1, \alpha_2, \alpha_3]$ denotes parameters of the fuel cost function.

The provision of regulation affects the operation of the industrial park in two aspects. First, the provision of regulation influences both the product revenue of the ASLs and the operational cost of thermal power plants. This influence has been considered in (2). Second, as ASLs operate at 95 percent of the rated power, the overload of ASLs for down-reserve regulation would increase the damage probability of the ASLs equipment. We define ξ as the maintenance cost and τ as the maintenance cycle of the ASLs. Let $\tau_{eco\%}$ denotes the maintenance cycle of ASLs operating at economic operation, i.e., 95 percent of the rated power, the maintenance cost in period $\tau_{eco\%}$ is ξ_{eco}. The higher output of the ASLs would increase the damage probability of the ASLs equipment, as a consequence, the maintenance cost fee $\xi_{h,j,t}$ is higher than that of $\xi_{eco,j}$. The difference between the two maintenance costs in each time slot denoted by $\eta_{h,j,t}^{regulation}$ can be expressed as:

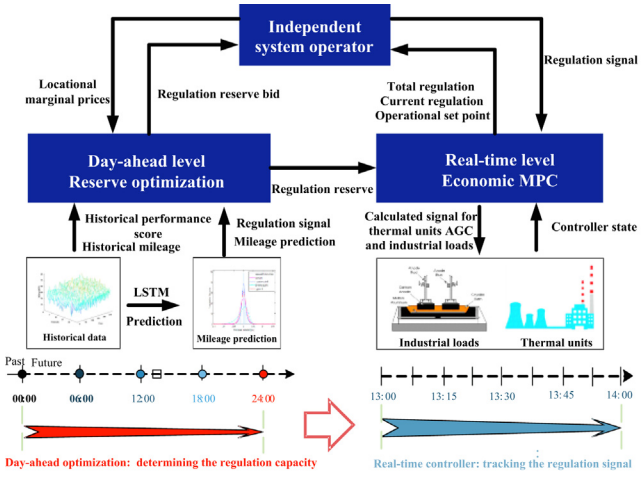

Fig. 2. Hierarchical controller for the industrial park.

$$\eta_{h,j,t}^{regulation} = \frac{\xi_{h,j,i} - \xi_{eco,j}}{\tau_{eco,j}} = \frac{\xi_{eco,j}(\tau_{h,j,t} - \tau_{eco,j})}{\tau_{eco,j}\tau_{h,j,t}} \tag{5}$$

If the operating power exceeds the economic point, this regulation process received an overload penalty which is formulated as:

$$\text{Penalty}_h^{regulation} = \sum_{j\in J}\sum_{t\in T}[\eta_{h,j,t}^{regulation}.\max\left(\frac{P_{h,j,t}^{load} - P_{eco,j}^{load}}{P_{eco,j}^{load}}, 0\right)\Delta t], \forall\, h, j, t \tag{6}$$

3.1.2. Constraints

The constraints are formulated as follows:

$$\sum_{i\in I} P_{h,i,t}^{generator} + K_i^{perf}\omega_{h,t}r_{h,t}^{reg} = \sum_{j\in J} p_{h,j,t}^{load}, \forall\, h, i, j, t \tag{7a}$$

$$-1 \leqslant \omega_{h,t} \leqslant 1, \forall\, h, t \tag{7b}$$

$$0 \leqslant r_{up,t}^{reg} \leqslant \sum_{i\in I}(P_{eco,i}^{generator} - P_{\min,i}^{generator}) + \sum_{k\in K}(P_{\max,k}^{load} - P_{eco,k}^{load}), \forall\, i, t, k \tag{7c}$$

$$0 \leqslant r_{down,t}^{reg} \leqslant \sum_{i\in I}(P_{\max,i}^{generator} - P_{i,eco}^{generator}) + \sum_{j\in J}(P_{eco,j}^{load} - P_{\min,j}^{load}), \forall\, i, t, j \tag{7d}$$

$$r_h^{reg} = r_h^{up} = r_h^{down}, \forall\, h, t \tag{7e}$$

$$P_{\min,i}^{generator} \leqslant P_{h,i,t}^{generator} \leqslant P_{\max,i}^{generator}, \forall\, h, t, i \tag{7f}$$

$$P_{\min,j}^{loads} \leqslant P_{h,j,t}^{loads} \leqslant P_{\max,j}^{loads}, \forall\, h, t, j \tag{7g}$$

$$\beta_{down,i}^{generator} P_{rate,i}^{generator} \leqslant P_{h,i,t}^{generator} - P_{h,i,t-1}^{generator} \leqslant \beta_{up,i}^{generator} P_{rate,i}^{generator}, \forall\, h, t, i \tag{7h}$$

$$\beta_{down,j}^{loads} P_{rate,j}^{loads} \leqslant P_{h,j,t}^{loads} - P_{h,j,t-1}^{loads} \leqslant \beta_{up,j}^{loads} P_{rate,j}^{loads}, \forall\, h, t, j \tag{7i}$$

Constraint (7a) is the power balance in the industrial park and $\omega_{h,t}$ is the regulation signal sent from ISO, such as PJM. The signal can take any value in $[-1,1]$ as expressed in (7b). The analysis of this signal is presented in the next part. Constraints (7c), (7d), and (7e) guarantee that the up-regulation reserve $r_{up,h}^{reg}$ and the down-regulation reserve $r_{down,h}^{reg}$ in each hour are equal. Constraints (7f) and (7 g) ensure that the power of the thermal power plants and the aluminum loads should not exceed the safe operating areas. Constraints (7 h) and (7i) are ramping limits of thermal power plants. The maximum loading rate for thermal power plants is on the order of 2 percent of maximum continuous rating (MCR) per minute [38]. For aluminum loads, this rate is on the order of 100 percent of MCR per minute.

3.1.3. Problem formulation

The reserve scheduling problem can be formulated as:

$$\underset{r_h^{reg}, P_{h,t,t}^{generation}, P_{h,k,t}^{load}}{\text{maximize}} \quad (1)$$
$$\text{subject to (7a) - (7i)} \tag{8}$$

3.2. Algorithm and implementation issues

3.2.1. Trajectory transition of the stochastic regulation signal

Notice that $\omega_{h,t}$ is a random signal that creates uncertainty for the regulation capacity. Meanwhile, it is difficult to directly model the regulation signal trajectories since there are a large number of possible trajectories. Ref. [24] studied that if the regulation resources can follow the regulation signal in two extreme cases, i.e., a trajectory with an extreme downward deviation from 1 to −1, and a trajectory with an extreme upward deviation from −1 to 1, the regulation resources can follow the regulation signal under other trajectories. However, as the ramp rate of industrial park regulation resources is limited, the number of extreme up and down deviations affects the regulation capacity. Hence, different from [24], this study is to deal with the stochastic regulation signal by replacing it with standard trajectories with different numbers of extreme up and down deviations. The different extremely trajectories is shown in the left plot in Fig. 3.

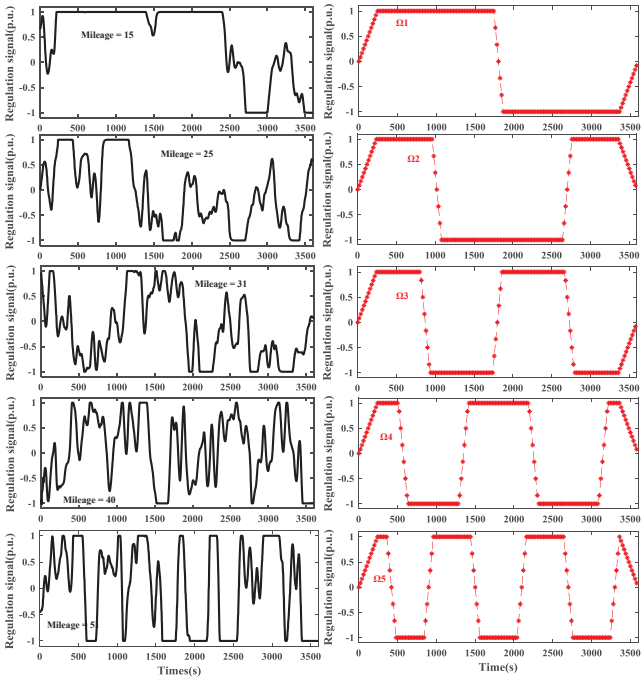

Fig. 3. Historical regulation mileage and extremely trajectories.

Here, the regulation mileage concept is used, and a regulation mileage is defined by PJM to characterize the fluctuation of a different regulation signal by the absolute sum of the regulation signal's movement [36]. The correlation between the real regulation signal and regulation mileage is shown in Fig. 3. A larger mileage corresponds to a more severe fluctuation as seen in Fig. 3. We sort the mileage of the regulation signal into different bins by amplitude i.e., a bin with mileage values from 10 p.u. to 60 p.u., which are denoted as [bin1, bin2, bin3, bin4, bin5]. Moreover, the trajectories that contain different numbers of extreme deviations are denoted as [Ω1, Ω2, Ω3, Ω4, Ω5]. By running numerical simulations using historical regulation signals and different numbers for extreme trajectories, the effect of the regulation mileage to the regulation reserve is characterized by the number of extreme deviation trajectories. The detailed relationship is presented in Section 6. In an alternative way, we utilize the trajectories Ω1, Ω2, Ω3, Ω4, Ω5 as the input regulation signal instead of the real regulation signal at each hour.

3.2.2. Prediction of regulation signal

The historical regulation signal mileage of PJM from March 1, 2017, to March 1, 2018, is presented in Fig. 4. By utilizing this historical data, the regulation signal mileage can be predicted by long short-term memory network (LSTM) prediction [37]. The persistence prediction uses the latest available observation as a prediction, and the mean prediction uses the average from all available observations as predictions. Hence, the corresponding trajectories Ω related to the predicted mileage can be obtained. Moreover, the random regulation signal $\omega_{h,t}$ is replaced by the trajectories Ω which contains a different number of extreme deviations in each hour.

3.2.3. Implement flowchart

By using regulation mileage, (8) is transformed into a deterministic optimization with a quadratic objective function, which can be solved

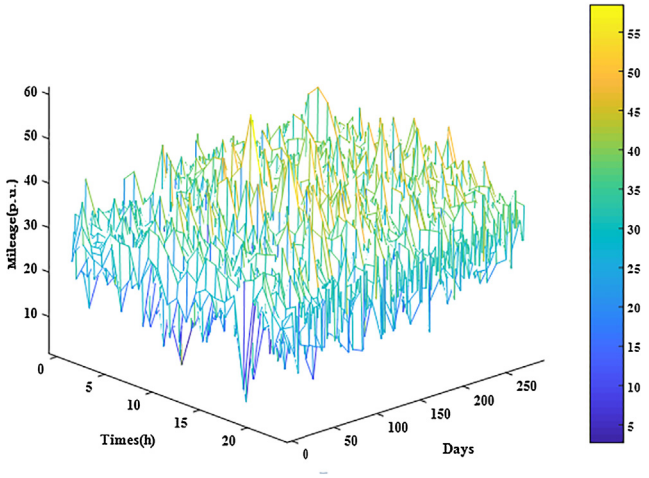

Fig. 4. Historical mileage of regulation signal.

by commercially available solvers such as CPLEX or YALMIP [38]. The flowchart of the day-ahead optimization schedule is shown in Fig. 5. The outcomes of (8) are reserve capacity, the thermal power plants' outputs, and the aluminum loads outputs, which are sent to the real-time operation controller for optimal dispatch.

4. Economic model predictive control for real-time operation

4.1. Dynamic model of the industrial park power system

4.1.1. Electrolysis loads model

Electrolysis loads all utilize the same process whereby cells are placed in series and heated by a large direct current. The equivalent circuit of aluminum smelter loads (ASLs) is shown in Fig. 6. The ASL is equal to the series connection of a counter electromotive force E and resistance R.

In our previous works, the dynamic model of ASLs has been obtained through field experiments [22] as shown in Fig. 7. The state space model with state variable $\Delta P_{ASL}(s)$ and the control variable ΔP_{ASLref} is expressed as follows:

$$[\Delta \dot{P}_{ASL}] = \left[\frac{1}{T_{ASL}}\right][\Delta P_{ASL}] + \left[\frac{K_{ASL}}{T_{ASL}}\right]\Delta P_{ASLref} \tag{9}$$

where parameters K_{ASL} and T_{ASL} can be found in [22].

4.1.2. Thermal power plant model

The state space model of the self-owned thermal power plants can be obtained directly from the block diagram [38]:

$$\Delta \dot{P}_{mi} = -\frac{1}{T_{ti}}\Delta P_{mi} + \frac{1}{T_{ti}}\Delta P_{gi} \tag{10}$$

$$\Delta \dot{P}_{gi} = -\frac{1}{T_{gi}R_i}\Delta f_i - \frac{1}{T_{gi}}\Delta P_{gi} + \frac{1}{T_{gi}}\Delta P_{Ci} \tag{11}$$

$$\Delta \dot{f}_i = -\frac{1}{D{\cdot}M_i}\Delta f_i - \frac{1}{M_i}\Delta P_{tie\,i} + \frac{1}{M_i}\Delta P_{mi} - \frac{1}{M_i}\Delta P_L \tag{12}$$

$$\Delta \dot{P}_{tie,12} = 2\pi T_{12}(\Delta f_1 - \Delta f_2) \tag{13}$$

where T_t and T_g are the time constants of the governor and the turbine of the thermal power plant, respectively, M is the inertia constant, D is the load damping constant, and R is the governor droop of the thermal power plant [38]. ΔP_m is the incremental mechanical power, ΔP_g is the incremental value gate position, Δf is the incremental frequency, ΔP_L is the incremental load demand, ΔP_C is the control signal of the thermal power plant, $\Delta P_{tie,12}$ is the incremental tie-line power, and T_{ij} is the interconnection gain between the industrial park and the bulk power grid. Δf_2 is the incremental frequency of the bulk power grid, and as the capacity of the bulk power grid can be regarded as infinite, $\int \Delta f_2$ is zero, hence (13) can be reformulated by:

$$\Delta \dot{P}_{tie,ij} = 2\pi T_{ij}(\Delta f_1) \tag{14}$$

ΔP_L consists of the incremental power of ASLs ΔP_{ASL} and incremental power of conventional loads ΔP_{CL} as:

$$\Delta P_L = \Delta P_{ASL} + \Delta P_{CL} \tag{15}$$

4.1.3. State space model of the industrial park

By combining (9–12) with (14) and (15), the discrete linear state space model of the industrial park can be uniformly described by the following equation:

$$\begin{aligned} \dot{x}_i(k+1) &= A_i x_i(k) + B_i u_i(k) - Ew(k) \\ y_i(k) &= Cx_i(k) \end{aligned} \tag{16}$$

where $x_i = [x_{Gi}; x_{ASLi}]$, $x_{Gi} = [\Delta P_m\ \Delta P_g\ \Delta f\ \Delta P_{tie}]^T$, $x_{ASLi} = [\Delta P_{ASLi}]^T$ is the state, $u_i = [u_{Gi}; u_{ASLi}]$, $u_{Gi} = [\Delta P_{Ci}\ ]^T$, $u_{ASLi} = [\Delta P_{ASLrefi}\ ]^T$ is the control variable, $w = \Delta P_{CLi}$ is the disturbance, and $y = [\Delta f\ \Delta P_{tie}]^T$ is the output vector of the industrial park. A, B, C, and E represent system matrices, which can be obtained using (9)–(15).

4.2. EMPC formulation

In this paper, we present an economic model predictive control (EMPC) scheme to overcome the conflict between regulation performance and the profits of industrial parks. The EMPC minimizes an economic cost directly as opposed to minimizing the deviation from the set point. The primary task of the EMPC is to decide which input variables should be actuated to realize the maximize profits from the frequency regulation services. Meanwhile, the controller should track the regulation signal as accurately as possible.

4.2.1. Objective of EMPC

Depending on the desires of the controller, the cost function of the EMPC contains five parts. The first part is the quadratic function for the deviation of a state from its steady-state value which indicates that the industrial loads follow the frequency regulation signal as committed. The second part and the third part denote the operating loss of the thermal power plants and the products profits loss of the ASLs,

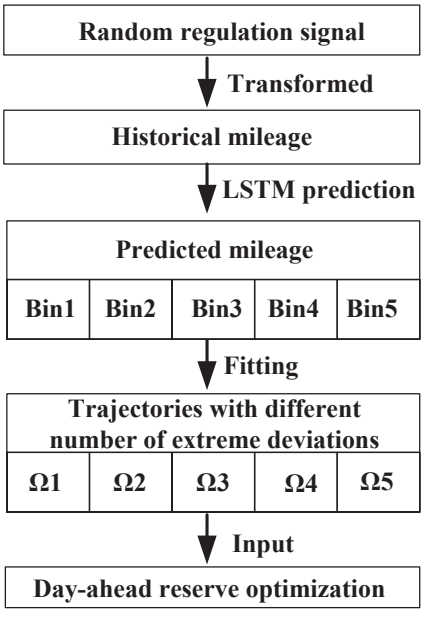

Fig. 5. Flowchart of day-ahead optimization schedule.

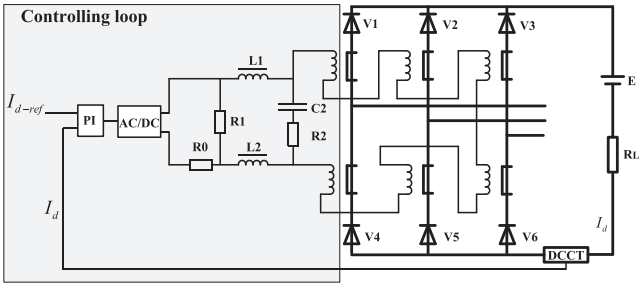

Fig. 6. The equivalent circuit of the ASL [18].

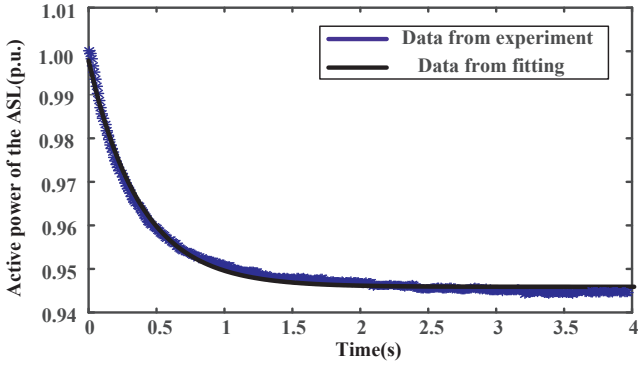

Fig. 7. Dynamic characteristics of ASLs from experiments [22].

respectively. The fourth part penalizes the deviation of consumption of its value in the previous time step which causes a smoother operation of the ASLs. The last part serves to penalize the overload of the ASLs. Taking into account the penalties above, the objective function of EMPC is formulated as:

$$\begin{aligned}\min\ J = &\sum_{n=0}^{N_2-1}(x_G^T(n+1)Q_{reg}x_G(n+1) + u_G^T(n)Q_G u_G(n)\\ &+ Q_{ASL}u_{ASL}(n) + \Delta u_{ASL}^T(n)Q_{varypenalty}\Delta u_{ASL}(n)\\ &+ Q_{overpenalty}\max(u_{ASL}(n),0))\end{aligned} \tag{17}$$

where Q_{reg}, Q_G, Q_{ASL} $Q_{varypenalty}$, and $Q_{overpenalty}$ are the weighting matrices corresponding to the regulation profit, generators energy losses, ASL products loss, variation penalty, and regulation penalty. u_{Gmin}, u_{Gmax}, u_{ASLmin}, and u_{ASLmax} are the amplitude constraints of the control variables of the thermal power plants and the ASLs. Δx_{Gmin}, Δx_{Gmax}, Δx_{ASLmin}, and Δx_{ASLmax} are the ramping constraints of the thermal power plants and the ASLs. N2 is the prediction horizon. As the real-time rolling forecast has a good performance [16]. Hence in our manuscript, the uncertainty of the regulation signal is not taken into consideration in real-time, and the latest information of the regulation signal is directly used in this EMPC model.

4.2.2. Constraints of EMPC

The constraints are formulated as follows:

$$x(n+1) = A_d x(n) + B_d u(n) \tag{18a}$$

$$u_{G\min} \leqslant u_G(n) \leqslant u_{G\max} \tag{18b}$$

$$u_{ASL\min} \leqslant u_G(n) \leqslant u_{ASL\max} \tag{18c}$$

$$x_{G\min} \leqslant x_G(n) \leqslant x_{G\max} \tag{18d}$$

$$x_{ASL\min} \leqslant x_{ASL}(n) \leqslant x_{ASL\max} \tag{18e}$$

$$\Delta x_{G\min} \leqslant \Delta x_G(n) \leqslant \Delta x_{G\max} \tag{18f}$$

Constraint (18a) is the model of MPC. It is the state space function of the industrial park power system presented in (16). Constraints (18b) and (18c) are the rate limits of the industrial loads and the thermal power plants. The maximum loading rate for thermal power plants is on the order of 2 percent of maximum continuous rating (MCR) per minute. For aluminum loads, this rate is on the order of 100 percent of MCR per minute. Constraints (18d) and (18e) ensure that the power of the thermal power plants and the aluminum loads does not exceed the safe operating areas. Constraint (18f) is the limit to the ramping rate of thermal power plants.

4.2.3. Formulation of EMPC

Combining (17) and (18), we can formulate the EMPC as below:

$$\begin{aligned}\min\ J = &\sum_{n=0}^{N_2-1}(x_G^T(n+1)Q_{reg}x_G(n+1) + u_G^T(n)Q_G u_G(n)\\ &+ Q_{ASL}u_{ASL}(n) + \Delta u_{ASL}^T(n)Q_{varypenalty}\Delta u_{ASL}(n)\\ &+ Q_{overpenalty}\max(u_{ASL}(n),0))\\ s.t.\ \ &x(n+1) = A_d x(n) + B_d u(n)\\ &u_{G\min} \leqslant u_G(n) \leqslant u_{G\max}\\ &u_{ASL\min} \leqslant u_G(n) \leqslant u_{ASL\max}\\ &x_{G\min} \leqslant x_G(n) \leqslant x_{G\max}\\ &x_{ASL\min} \leqslant x_{ASL}(n) \leqslant x_{ASL\max}\\ &\Delta x_{G\min} \leqslant \Delta x_G(n) \leqslant \Delta x_{G\max}\\ &\forall\ n = 0, 1, \cdots, N_2 - 1\end{aligned} \tag{19}$$

The EMPC solved in this paper is formulated as a convex quadratic problem that can be solved by YALMIP [39]. The solution to (19) is denoted $U^* = \{u_{k+j}^*\}_{j=0}^{N-1}$, and the first element will be returned as the optimal power plan for thermal plants and aluminum loads.

5. Case study

5.1. Simulation system

In this section, we validate the framework's performance in a typical industrial park with ASLs and thermal power plants. We consider that the industrial park has one series of aluminum loads with a capacity of 500 MW, and two self-owned thermal power plants with a capacity of 600 MW. The industrial park power system is connected to the bulk power system through a tie-line. The detailed parameters of the industrial park are listed in Table 2.

The income of the industrial park is equal to its production benefits subtracted by the operation cost of its thermal power plants. The power

Table 2
System parameters of the industrial park.

Description	Parameter	Value
Day-ahead level	$P_{eco}^{generatot}$	490 MW
	P_{eco}^{load}	490 MW
	$P_{\min}^{load}$	400 MW
	$P_{\max}^{load}$	500 MW
	$\beta_{up}^{genarotar}$	2%/min
	$\beta_{down}^{genarotar}$	5%/min
	β_{up}^{load}	50%/min
	$\beta_{down}^{genarotar}$	50%/min
	π^{cap}	$51.36/MW
	π^{perf}	$3.72/MW
	$\pi^{product}$	$2044/ton
	$\eta^{product}$	$200/MW
Real-time level	T_t	10
	T_g	2
	M	10
	D	1
	N_2	300 s
	$u_{ASL\min}$, $u_{ASL\max}$	−20%|0%
	$\Delta x_{G\min}$, $\Delta x_{G\max}$	−5%/min|2%/min
	Q_{reg}, Q_G, Q_{ASL}, $Q_{vpenalty}$, $Q_{overpenalty}$	[100, 62, 70, 30, 200]

consumption of ASLs requires the thermal power plants to operate at 95 percent load factor with limited perturbation within an hour, and the industrial park's nominal power production rate is 1700 tons per hour. The average price of aluminum production is $2044/ton. To investigate the framework's performance, we use the average regulation capacity price and the average regulation performance price of PJM on October 8, 2017, and the regulation signal from October 8, 2017, to October 13, 2017. The sampling time of the regulation signal is every 2 s. The average mileage ratio of the regulation signal is 2.92.

Simulations are performed in MATLAB by calling YALMIP to solve the optimization problem [39]. The reserve scheduling problem is solved with 24-hour time slots and 5 min time steps in each hour. The real-time control problem is solved with a 300s prediction time horizon and a time step of 2 s. This predictive horizon is based on the PJM power market [40]. And the proposed EMPC method is compared with the traditional MPC whose objective is focused on tracking the regulation performance. In addition, the hierarchical control method is also verified when there is the prediction error of day ahead regulation capacity.

5.2. Day-ahead capacity reserve schedule

To quantify the correlation between regulation mileage and regulation reserve, we run numerical simulations with real regulation signals across several months. The results shown in Fig. 8 indicate that regulation reserve is highly related to mileage. When mileage is high, the regulation reserve is low. The black rectangles in Fig. 9 denote regulation reserve with different numbers for extremely deviated regulation signals. In each mileage bin, the average regulation reserve as calculated by the real regulation signal is approximately the same as it is under extremely different deviation trajectories. The average regulation reserve for each mileage bin is listed in Table 3.

Then we predict the day-ahead mileages. The daily regulation mileage signal for the simulation is plotted in Fig. 10 together with the LSTM prediction. As shown in Fig. 10, the root-mean-square-error (RMSE) is 5.2953 MW.

Utilizing the relationships in Table 3 and the predicted mileage, we solve the day-ahead reserve schedule problem. The optimization results for each hour of the next operating day are shown in Fig. 11. The black-solid and black-dashed curves indicate the predicted mileage and the real mileage of the regulation signal. The blue bar represents the regulation reserve based on the predicted mileage, and the gray-dotted curves represent the regulation reserve based on the real regulation signal. The graph in Fig. 11 indicates that the regulation reserve of an industrial park with 500 MW capacity is more than 30 MW, and the average net profit compared with the income without regulation is $2450. Moreover, the PJM's regulation requirement is 700 MW during peak periods and 525 MW during off-peak periods in PJM. Hence, the amount of regulation reserve provided by the industrial park can contribute to this frequency regulation market.

Note that there exists some error between the mileage-based regulation reserve and the actual signal-based regulation reserve. This error, shown in Fig. 10, results from a prediction error in mileage and would influence real-time operation results. Hence, in the second part of the case study, we present real-time operation results with a consideration of the influence of this prediction error.

5.3. Real-time regulation ignore the day-ahead prediction error

The real-time regulation simulation is investigated to demonstrate the effectiveness of the proposed EMPC for optimal dispatch of the industrial park. The proposed framework is compared with the traditional MPC in terms of tracking performance and regulation economics.

The results are presented in Figs. 12 and 13. The red curve in Fig. 12 is the hourly dynamic regulation signal. The black curves in Figs. 12 and 13 represents the dynamic response of the active power of the industrial park, the industrial loads and the thermal power plant based on EMPC and the red curves in Fig. A1, Fig. 12 and Fig. 13 represents the dynamic response of the active power of the industrial park, the industrial loads and the thermal power plant based on traditional MPC. As the regulation signal changes, the thermal power plants and the industrial loads respond to track it. Due to the limit of the governed dynamic, the thermal power plants are slow to track the regulation signal. Hence, the industrial loads respond quickly to follow the regulation signal followed by the change of thermal power plants. By coordinating thermal power plants and industrial loads, the industrial park can track the regulation signal well. The performance score of this regulation is 0.90.

The most significant difference between traditional MPC and economic MPC is the dynamic response of industrial loads, especially in the periods when industrial loads go down or up. As seen in the period t = 450:500, the regulation signal ramps extremely fast from −1 p.u. to 1 p.u. in 1 min. In the traditional MPC strategy, the output of industrial loads decreases rapidly to help industrial park keep track of the regulation signal. While the reduction of industrial load in economic MPC is less which causes a lower regulation performance. In the period t = 2400:2700 when the reference signal goes up in an extreme fashion, the output of industrial loads increases to keep track of the regulation signal in the traditional MPC strategy as seen in Fig. 13. In economic MPC strategy, there is a penalty for overloading industrial load's that would increase the risk of equipment failures. Hence, the industrial loads' overload time is shorter in economic MPC than that in traditional MPC. Fig. 14 compares the economic benefits of traditional MPC and economic MPC. From Fig. 14, although the regulation income with traditional MPC is higher than the economic MPC, the total net income of economic MPC is higher than the net income of traditional MPC. The proposed EMPC brings more revenue than the traditional MPC due to a less stringent regulation penalty. The detail economic benefits of traditional MPC and economic MPC are listed in Table 4.

5.4. Performance verification of the hierarchical framework considering day-ahead prediction error

The prediction error of regulation reserve would influence the total income of the industrial park in the real-time operation. For example, when the fluctuation of the real regulation signal is more severe than the fluctuation of the predicted signal, if we pursue the same performance score, a more variation of the industrial loads is required which would affect the final regulation income of the industrial park. Consequently, the prediction error requires to be considered in the real-time regulation (Fig. 15).

In this scenario, we consider the extreme case. The day-ahead reserve schedule calculates the optimal regulation reserve is 45 MW with a predicted regulation mileage. However, the actual regulation mileage is higher than the predicted one, and the actual optimal regulation capacity would be 25 MW. We compare the proposed framework with the traditional MPC in terms of tracking performance and regulation economics.

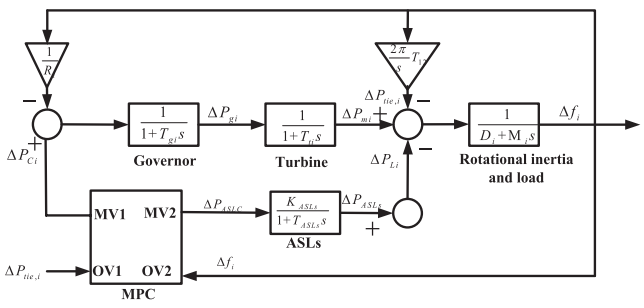

Fig. 8. The considered power system model of the industrial park.

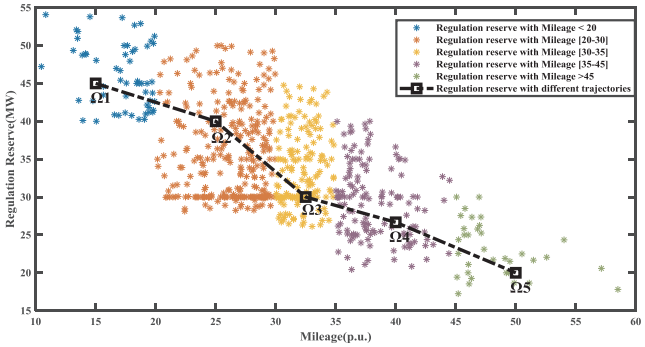

Fig. 9. Relationship between regulation reserve and mileage.

Table 3
Relationship between regulation reserve and mileage.

Mileage (p.u.)	Regulation reserve (MW)	Number of ramp events
< 20	45	1
20–30	40	2
30–35	30	3
35–45	26.7	4
> 45	20	5

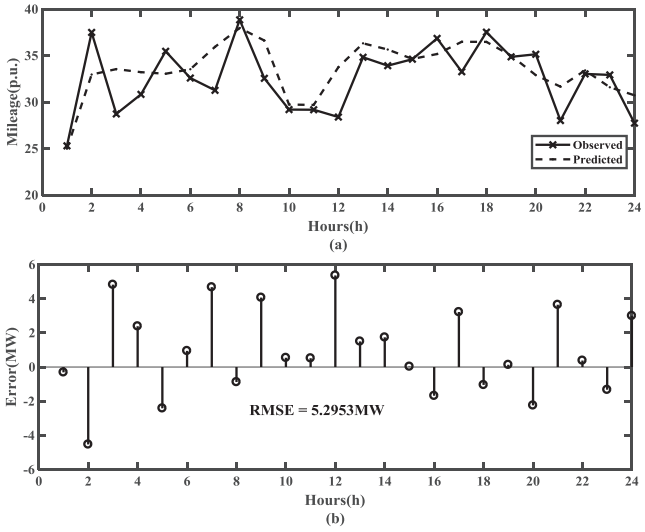

Fig. 10. Regulation mileage over five days and its prediction.

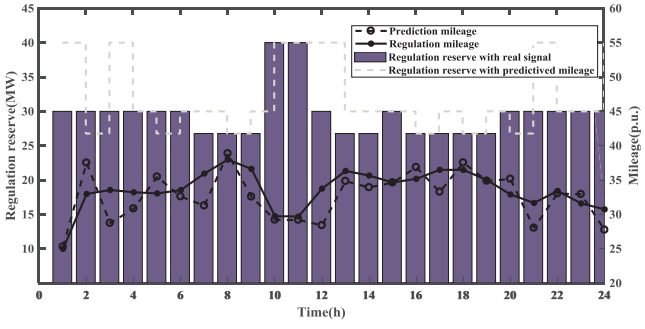

Fig. 11. Day-ahead scheduling result.

Regulation results with 25 MW regulation reserve are shown in Figs. 16 and 17. The red curve in Fig. 16 is the real regulation signal. The black and the blue curves in Fig. 16 denote the output of the industrial park with traditional MPC and economic MPC. The black and the blue curves in Fig. 17 show the dynamic response of industrial loads

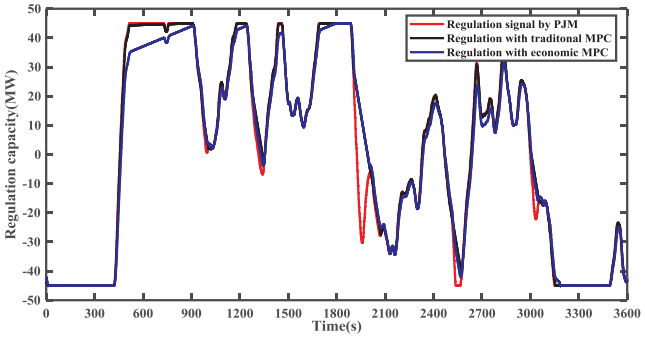

Fig. 12. Hourly simulation results of regulation signal.

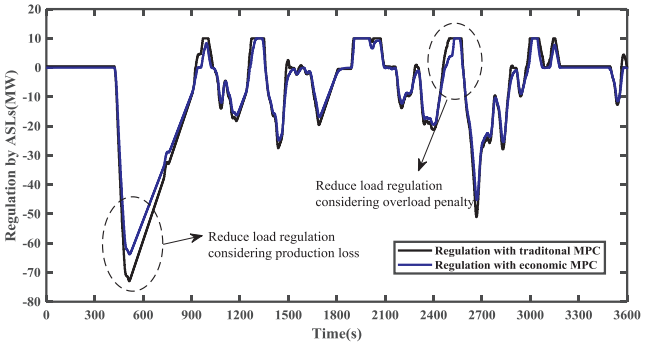

Fig. 13. Hourly simulation results of industrial loads.

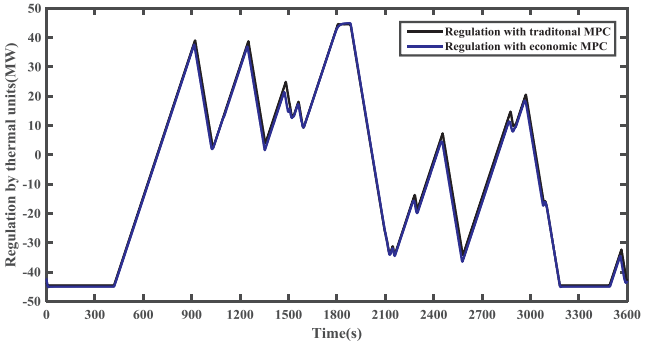

Fig. 14. Hourly simulation results of thermal power plants.

Table 4
Comparison of system operation cost between traditional MPC and Economic MPC.

	Traditional MPC	Economic MPC
Total net income ($)	2000	3613
Regulation income ($)	10,926	10,374
Production loss ($)	2822	2774
Generation cost ($)	140	162
Regulation penalty ($)	6245	4147

with traditional MPC and economic MPC. Regulation results with 45 MW regulation reserve are shown in Figs. 18 and 19. The red curve in Fig. 18 is the real regulation signal. The black and the blue curves in Fig. 18 denote the output of the industrial park with traditional MPC and economic MPC. The black and the blue curves in Fig. 19 show the dynamic response of industrial loads with traditional MPC and economic MPC.

When the regulation reserve is 25 MW based on the real mileage, both the traditional MPC and the economic MPC are profitable. However, there are also some differences marked as the dotted circles

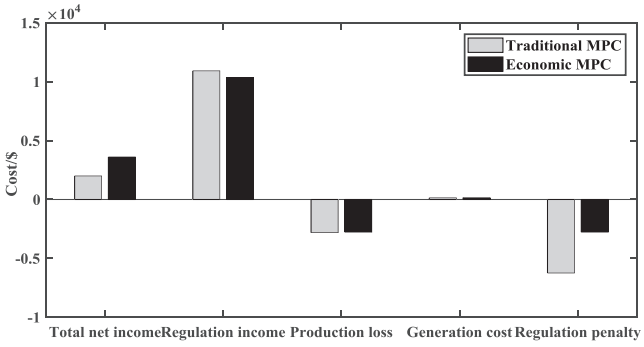

Fig. 15. Hourly simulation results.

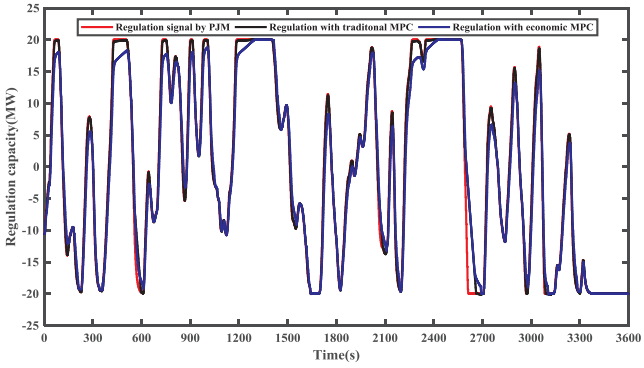

Fig. 16. Hourly simulation results of industrial parks with a 25 MW regulation capacity.

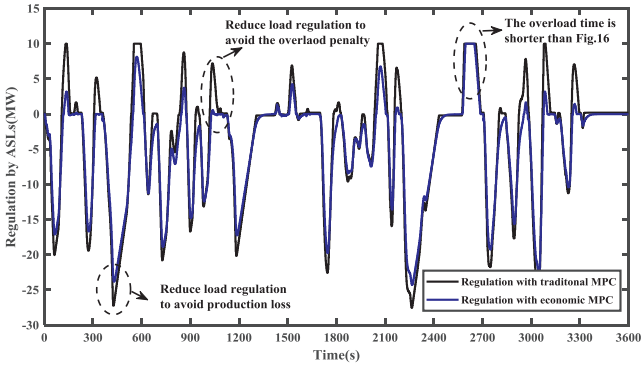

Fig. 17. Hourly simulation results of industrial loads a 25 MW regulation capacity.

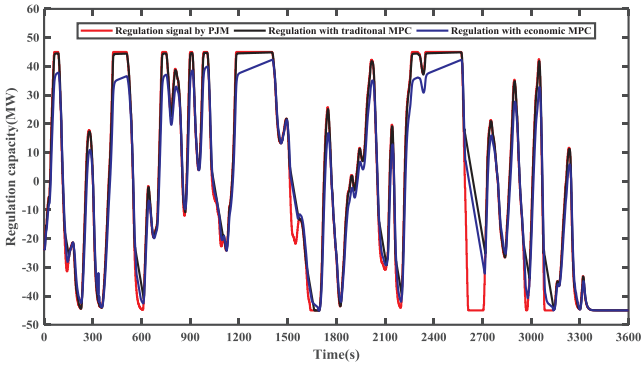

Fig. 18. Hourly simulation results of industrial parks with a 50 MW regulation capacity.

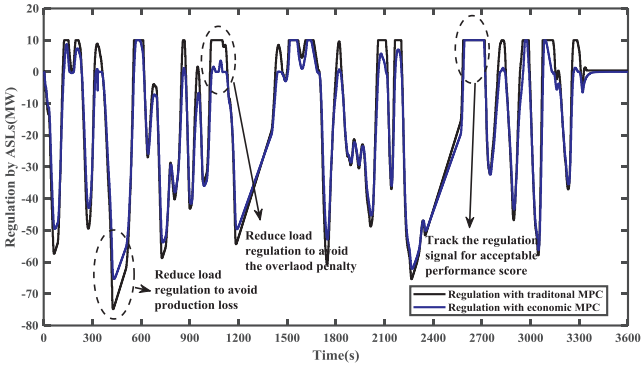

Fig. 19. Hourly simulation results of industrial loads a 50 MW regulation capacity.

Table 5
Comparison of system operation cost.

Cost ($)	Traditional MPC		Economic MPC	
	R = 20 MW	R = 45 MW	R = 20 MW	R = 45 MW
Total income ($)	627	−3061	1502	941
Regulation income ($)	4803	10,145	4424	9285
Production loss ($)	2065	4086	2159	4287
Generation cost ($)	78	290	100	384
Regulation penalty ($)	2188	9409	862.7	4441
Performance score	0.933	0.876	0.860	0.810

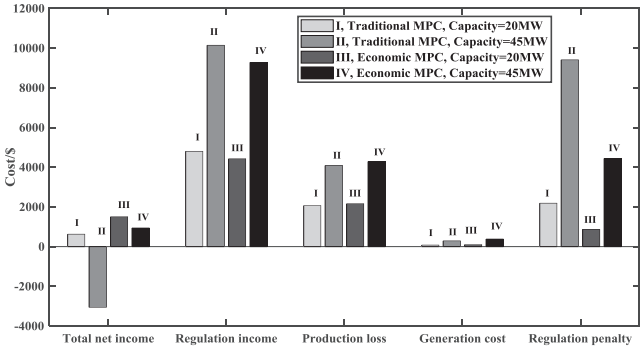

Fig. 20. Economic results of industrial parks with a 50 MW regulation capacity.

in Fig. 17. The deviation amplitude of industrial loads in EMPC is lower than the traditional MPC. In the time period of t = 900 s to 1200 s, the output of industrial loads goes up to help track the regulation signal in the traditional MPC. However, the output of industrial loads almost keeps its normal operation?? Both of these controllers can get a high-performance score as listed in Table 5. However, the total net income of the economic MPC is higher than the traditional MPC as shown in Fig. 20.

When the regulation capacity is 45 MW which is based on the predicted mileage, the difference of the traditional MPC and the economic MPC is revealed. The tracking performance in the traditional MPC is still higher than the economic MPC. However, the high regulation performance compromises more production profits due to energy loss and more regulation penalties due to the overloading of industrial loads. Hence the total net income of economic MPC is much higher than the traditional MPC. Moreover, the regulation performance of the economic MPC is higher than the basic requirement of PJM whose minimal regulation performance score is 0.75. The detail economic benefits of traditional MPC and economic MPC are listed in Table 5.

6. Conclusions

This paper presents a hierarchical framework to coordinate thermal power plants and industrial loads in the industrial park for frequency regulation. The framework consists of the day-ahead regulation reserve optimization and a real-time model predictive controller. By utilizing the mileage feature of the regulation signal, the random regulation signal is transformed into a deterministic optimization, and the regulation reserve of each operating hour is optimized. The utilization of economic model predictive control achieves the maximum benefit to the industrial park through participation in the frequency regulation. The operation simulation in this study demonstrates the flexibility of industrial parks for frequency regulation. By utilizing the proposed framework, the economics of industrial parks during frequency regulation is optimized while the electricity service is maintained. Even though the study is based on ASL, the proposed framework also works for other types of industrial electrolysis loads.

Future work should address the uncertainty of market prices in detail. The bidding model of industrial parks for frequency regulation also needs to be developed. Utilization of other energy-intensive loads, e.g., steel loads and arc furnace loads, for frequency regulation will be studied in the near future.

References

[1] Federal Energy Regulatory Commission (FERC). FERC Order 755: Frequency Regulation Compensation in the Organized Wholesale Power Markets. Tech Rep: 2011.

[2] National id National Grid. Enhanced frequency regulation response: invitation to tender for pre-qualified parties: 2016. http://www2.nationalgrid.com/Enhanced-Frequency-Response.aspx.

[3] National Energy Administration of China. Notice on the promotion of electric energy storage to participate in the electric ancillary service compensation mechanism in the north China: 2016 [in Chinese].

[4] National Development and Reform Commission of China, National Energy Administration of China. Notice on further improving the trading mechanism of electric power market transaction: 2018 [in Chinese].

[5] Liu H, Hu Z, Song Y, Lin J. Decentralized Vehicle-to-grid control for primary frequency regulation considering charging demands. IEEE Trans Power Syst 2013;28(3):1–10.

[6] Liu H, Qi J, Wang J, Li P, Li C. EV dispatch control for supplementary frequency regulation considering the expectation of EV owners. IEEE Trans Smart Grid 2018;9(4):3763–72.

[7] Liu H, Wang B, Wang N, Wu Q, Yang Y, Wei H, et al. Enabling strategies of electric vehicles for under frequency load shedding. Appl Energy 2018;228:843–51.

[8] Nicholas DF, Jason SM, Douglas RB. Day ahead optimization of an electric vehicle fleet providing ancillary services in the Los Angeles Air Force Base vehicle-to-grid demonstration. Appl Energy 2018;210:987–1001.

[9] Greenwood DM, Lim KY, Patsios C, Lydons PF, Lim YS, Taylor PC. Frequency response services designed for energy storage. Appl Energy 2017;203:115–27.

[10] Lakshmanan V, Marinelli M, Hu J, Bindner HW. Provision of secondary frequency control via demand response activation on thermostatically controlled loads: solutions and experiences from Denmark. Appl Energy 2016;173:470–80.

[11] Kondoh J, Lu N, Hammerstrom DJ. An evaluation of the water heater load potential for providing regulation service. IEEE Trans Power Syst 2011;26(3):1309–16.

[12] Lin Y, Barooah P, Meyn S, Middelkoop T. Experimental evaluation of frequency regulation from commercial building HVAC systems. IEEE Trans Smart Grid 2015;6(2):776–83.

[13] Shoreh MH, Siano P, Shafie-khah M, Loia V, Catalão JP. A survey of industrial applications of demand response. Electric Power Syst Res 2016;141:31–49.

[14] Alapera I, Honkapuro S, Paananen J. Data centers as a source of dynamic flexibility in smart girds. Appl Energy 2018;229:69–79.

[15] Li S, Brocanelli M, Zhang W, Wang X. Integrated power management of data centers and electric vehicles for energy and regulation market participation. IEEE Trans Smart Grid 2014;5:2283–94.

[16] Zhang X, Hug G, Kolter JZ, Harjunkoski I. Demand response of ancillary service from industrial loads coordinated with energy storage. IEEE Trans Power Syst 2018;33(1):951–61.

[17] Todd D, Caufield M, Helms B, Starke M, Kirby B, Kueck J. Providing reliability services through demand response: a preliminary evaluation of the demand response capabilities of Alcoa Inc Technical report. Alcoa Power Generating, Inc; Oak Ridge National Laboratory; 2009 [ORNL/TM-2008/233].

[18] Xu J, Liao S, Sun Y, Ma X, Gao W, Li X, et al. An isolated industrial power system driven by wind-coal power for aluminum productions: a case study of frequency control. IEEE Trans Power Syst 2015;30(1):471–83.

[19] Liao S, Xu J, Sun Y, Bao Y. Local utilization of wind electricity in isolated power systems by employing coordinated control scheme of industrial energy-intensive load. Appl Energy 2018;217:14–24.

[20] Jiang H, Lin J, Song Y, Gao W, Xu Y, Shu B, et al. Demand side frequency control scheme in an isolated wind power system for industrial aluminum smelting production. IEEE Trans Power Syst 2014;29(2):844–53.

[21] Sun Y, Liao S, Xu J, Gu R, Bao Y. Industrial implementation of a wide area measurement system based control scheme in an isolated power system driven by wind–coal power for aluminum productions. IET Gener, Transm Dis 2016;10(8):1877–82.

[22] Bao Y, Xu J, Liao S, Sun Y, Li X, Jiang Y, et al. Field verification of frequency control by energy-intensive loads for isolated power systems with high penetration of wind power. IEEE Trans Power Syst 2018.

[23] Zhao X. Approaches to enable demand response by industrial loads for ancillary services provision. Diss. Carnegie Mellon University: 2017.

[24] Donadee J, Ilić MD. Stochastic optimization of grid to vehicle frequency regulation capacity bids. IEEE Trans Smart Grid 2014;5(2):1061–9.

[25] Vagropoulos SI, Bakirtzis AG. Optimal bidding strategy for electric vehicle aggregators in electricity markets. IEEE Trans on Power Syst 2013;28(4):4031–41.

[26] Yao E, Wong VW, Schober R. Robust frequency regulation capacity scheduling algorithm for electric vehicles. IEEE Trans Smart Grid 2017;8(2):984–97.

[27] Vrettos E, Oldewurtel F, Andersson G. Robust energy-constrained frequency reserves from aggregations of commercial buildings. IEEE Trans Power Syst 2016;31(6):4272–85.

[28] Vrettos E, Andersson G. Scheduling and provision of secondary frequency reserves by aggregations of commercial buildings. IEEE Trans Sustain Energy 2016;7(2):850–64.

[29] Vrettos E, Kara EC, MacDonald J, Andersson G, Callaway DS. Experimental demonstration of frequency regulation by commercial buildings–Part I: Modeling and hierarchical control design. IEEE Trans on Smart Grid 2016.

[30] Vrettos E, Kara EC, MacDonald J, Andersson G, Callaway DS. Experimental demonstration of frequency regulation by commercial buildings–Part II: results and performance evaluation. IEEE Trans Smart Grid 2016.

[31] Galus MD, Koch S, Andersson G. Provision of load frequency control by PHEVs, controllable loads, and a cogeneration unit. IEEE Trans Ind Electron 2011;58(10):4568–82.

[32] Elsisi M, Soliman M, Aboelela MA, Mansour W. Model predictive control of plug-in hybrid electric vehicles for frequency regulation in a smart grid. IET Gener, Transm Dis 2017;11(16):3974–83.

[33] Ellis M, Durand H, Christofides PD. A tutorial review of economic model predictive control methods. J Process Contr 2014;24(8):1156–78.

[34] Chen X, Heidarinejad M, Liu J, Christofides PD. Distributed economic MPC: Application to a nonlinear chemical process network. J Process Contr 2012;22(4):689–99.

[35] Ma J, Qin SJ, Salsbury T. Application of economic MPC to the energy and demand minimization of a commercial building. J Process Contr 2014;24(8):1282–91.

[36] PJM Manual 11: Energy and Ancillary Services Market Operations, Rev. 62, PJM, Audubon, PA, USA, Dec. 2013.

[37] Greff K, Srivastava RK, Koutník J, Steunebrink BR, Schmidhuber J. LSTM: A search space odyssey. IEEE Trans Neur Net Lear Syst 2017;28(10):2222–32.

[38] Kundur P, Balu NJ, Lauby MG. Power system stability and control. New York: McGraw-hill; 1994.

[39] Lofberg J. YALMIP: a toolbox for modeling and optimization in MATLAB. IEEE international symposium on computer aided control systems design. 2004. p. 284–9.

[40] PJM Manual 28: Operating Agreement Acounting, PJM, Valley Forge, PA, USA, 2016.